The Astrophysical Journal, 693:1484–1493, 2009 March 10 doi:10.1088/0004-637X/693/2/1484

DARK BURSTS IN THE *SWIFT* ERA: THE PALOMAR 60 INCH-*SWIFT* EARLY OPTICAL AFTERGLOW CATALOG

S. B. Cenko[1,2], J. Kelemen[3], F. A. Harrison[1], D. B. Fox[4], S. R. Kulkarni[5], M. M. Kasliwal[5], E. O. Ofek[5], A. Rau[5], A. Gal-Yam[6], D. A. Frail[7], and D.-S. Moon[8]

[1] Space Radiation Laboratory, MS 220-47, California Institute of Technology, Pasadena, CA 91125, USA; cenko@astro.berkeley.edu
[2] Department of Astronomy, 601 Campbell Hall, University of California, Berkeley, CA 94720, USA
[3] Konkoly Observatory, H-1525, Box 67, Budapest, Hungary
[4] Department of Astronomy & Astrophysics, 525 Davey Laboratory, Pennsylvania State University, University Park, PA 16802, USA
[5] Department of Astronomy, Mail Stop 105-24, California Institute of Technology, Pasadena, CA 91125, USA
[6] Benoziyo Center for Astrophysics, Weizmann Institute of Science, Rehovot 76100, Israel
[7] National Radio Astronomy Observatory, P.O. Box 0, 1003 Lopezville Road, Socorro, NM 87801, USA
[8] Department of Astronomy and Astrophysics, University of Toronto, 50 St. George Street, Toronto, ON M5S 3H4, Canada
Received 2008 June 26; accepted 2008 September 12; published 2009 March 9

ABSTRACT

We present multicolor optical observations of long-duration γ-ray bursts (GRBs) made over a three-year period with the robotic Palomar 60 inch telescope (P60). Our sample consists of all 29 events discovered by *Swift* for which P60 began observations less than 1 hr after the burst trigger. We were able to recover 80% of the optical afterglows from this prompt sample, and we attribute this high efficiency to our red coverage. Like Melandri et al. (2008), we find that a significant fraction ($\approx$ 50%) of *Swift* events show a suppression of the optical flux with regard to the X-ray emission (the so-called "dark" bursts). Our multicolor photometry demonstrates this is likely due in large part to extinction in the host galaxy. We argue that previous studies, by selecting only the brightest and best-sampled optical afterglows, have significantly underestimated the amount of dust present in typical GRB environments.
Key words: gamma rays: bursts
Online-only material: color figures, machine-readable table

1. INTRODUCTION

The launch of the *Swift* γ-Ray Burst (GRB) Explorer (Gehrels et al. 2004) in 2004 November has ushered in a new era in the study of GRB afterglows. *Swift* offers a unique combination of event rate ($\sim$100 yr^{-1}; almost an order of magnitude increase over previous missions) and precise localization ($\sim$ 3′ radius error circles are distributed seconds after the burst, and refined to $\sim$ 3″ minutes later). The onboard X-ray Telescope (XRT; Burrows et al. 2005a) and the UV-Optical Telescope (UVOT; Roming et al. 2005), together with the rapid relay of these precise localizations to ground-based observers, have enabled an unprecedented glimpse into the time period immediately following the prompt emission over a broad frequency range.

Observations of X-ray afterglows with the XRT have generated particular interest in recent years. In the pre-*Swift* era, X-ray observations were limited to hours or days after the prompt emission, and were often poorly sampled compared with the optical and radio bandpasses. Routine XRT observations of *Swift* GRBs beginning at early times have revealed a central engine capable of injecting energy into the forward shock at times well beyond the duration of the prompt emission (e.g., Burrows et al. 2005b; Zhang et al. 2006). This discovery has had a profound effect on our understanding of progenitor models.

While the X-ray afterglow is currently a well-explored phase space, comparatively few analogous studies have been performed in the optical bandpass. Berger et al. (2005) first suggested that *Swift* optical afterglows were 1.8 mag fainter in the *R* band than pre-*Swift* events (at a common epoch of 12 hr after the burst). Likewise, Roming et al. (2006) found that only six of the first 19 *Swift* bursts with prompt ($\Delta t \lesssim 100$ s) UVOT coverage yielded optical afterglow detections. Since then, explaining the faintness of *Swift* optical afterglows has remained one of the outstanding questions in the field.

One clear contributor is distance: the median redshift of *Swift* events ($\langle z_{Swift} \rangle \approx 2.0$)[9] is significantly larger than the pre-*Swift* sample ($\langle z_{\mathrm{pre}-Swift} \rangle = 1.1$; Berger et al. 2005; Jakobsson et al. 2006b). In a comprehensive literature-based study of the brightest, best-studied *Swift* afterglows, Kann et al. (2007) found properties broadly similar to pre-*Swift* events, after applying a cosmological k-correction.

On the other hand, Melandri et al. (2008) have recently presented a sample of 63 GRBs observed in the optical (r' band) with the robotic 2 m Liverpool Telescope and Faulkes Telescopes (North and South). The selection criteria for including a burst in their sample are never explicitly stated, and several non-*Swift* bursts are included, making a direct comparison with the results of Kann et al. (2007) difficult. However, Melandri et al. (2008) do not exclude the significant fraction of events without optical detections from their analysis, providing a more unbiased look at optical afterglow properties. By measuring the ratio of optical to X-ray flux at a common time, these authors find that roughly half of the GRBs in their sample exhibit a relative suppression of the optical flux inconsistent with our standard picture of afterglow emission (e.g., Sari et al. 1998), the so-called "dark" bursts (Jakobsson et al. 2004). This finding suggests that distance alone cannot explain the faintness of *Swift* optical afterglows.

Several other possibilities have been suggested to explain optically dark GRB afterglows. Undoubtedly some GRBs, such as GRB 050904 (Haislip et al. 2006; Kawai et al. 2006), originate from such large redshifts ($z \gtrsim 6$) that Ly-α absorption in the intergalactic medium (IGM) completely suppresses the optical flux (Lamb & Reichart 2000). Alternatively, late-time energy injection from the central engine, manifested as bright X-ray

[9] Calculated from J. Greiner's compilation at http://www.mpe.mpg.de/~jcg/grbgen.html.

Table 1
P60-*Swift* Early Optical Afterglow Catalog

GRB Name	UT Date[a]	Time Since Burst[b] (s)	Filter	Exposure Time (s)	Magnitude	Photometric Calibration[c]
GRB 050412	2005 Apr 12.2431	391.0	R_C	60.0	> 20.8	1
...	2005 Apr 12.2468	684.7	R_C	180.0	> 21.4	...
...	2005 Apr 12.2512	1063.7	i	180.0	> 21.0	...
...	2005 Apr 12.2580	1646.0	z	180.0	> 20.2	...
...	2005 Apr 12.2720	2858.8	R_C	960.0	> 22.5	...
...	2005 Apr 12.2831	2817.0	i	960.0	> 22.0	...

Notes.
[a] UT at beginning of exposure.
[b] Time from mid-point of exposure to *Swift*-BAT trigger.
[c] References: 1 – SDSS; 2 – ftp.aavso.org; 3 – USNO-B1; 4 – Perley et al. (2008); 5 – Covino et al. (2008).
[d] Reference: Soderberg et al. (2007).
[e] Reference: Cenko et al. (2006b).
[f] Reference: Perley et al. (2008).
(This table is available in its entirety in a machine-readable form in the online journal. A portion is shown here for guidance regarding its form and content.)

flares and/or extended periods of shallow decay, may be artificially increasing the X-ray flux, leading to spurious claims of optically dark GRBs (Melandri et al. 2008).

One final possibility is extinction native to the GRB host galaxy. As a population, long-duration GRB host galaxies exhibit extremely large neutral H column densities (e.g., Hjorth et al. 2003; Berger et al. 2006), typically falling at $\log N_H > 20.3$ cm^{-2} (the so-called Damped Ly-α, or DLA systems; Wolfe et al. 2005). And within their hosts, GRBs trace the blue light from hot young stars in the disk even more closely than core-collapse supernovae (Bloom et al. 2002; Fruchter et al. 2006). Both findings are consistent with the observed association between long-duration GRBs and massive star death (e.g., Woosley & Bloom 2006).

In spite of these expectations, relatively few GRB afterglows to date exhibit signs of large host galaxy extinction (e.g., Castro-Tirado et al. 2007; Rol et al. 2007; Tanvir et al. 2008). Kann et al. (2007) found only a modest amount of dust ($\langle A_V \rangle = 0.20$ mag) for the 15 events in their "golden" sample, an identical value found from an analogous study of pre-*Swift* afterglows (Kann et al. 2006). The primary drawback of such studies, however, is the large and uncertain role of selection effects: by including only the brightest, best-sampled optical afterglows, Kann et al. (2007) may be preferentially selecting those events in low-extinction environments. Understanding these selection effects is one of the primary goals of this work.

The Palomar 60 inch telescope (P60) is a robotic, queue-scheduled facility dedicated to rapid-response observations of GRBs and other transient events (Cenko et al. 2006a). With a response time of $\Delta t \lesssim 3$ min and a limiting magnitude of $R \gtrsim 20.5$ (60 s exposure), the P60 aperture is well suited to detect most *Swift* optical afterglows (Akerlof & Swan 2007). In addition, with a broadband filter wheel providing coverage from the near-UV to the near-IR (NIR), P60 can also provide multicolor data on the afterglow evolution.

In this work, we present the P60-*Swift* early optical afterglow sample: 29 unambiguously long-duration GRBs detected by the *Swift* Burst Alert Telescope (BAT; Barthelmy et al. 2005) with P60 observations beginning at most 1 hr after the burst trigger time. This sample offers two distinct advantages over previous efforts to understand the optical afterglow emission from GRBs. First and foremost, our study enforces a strict selection criterion independent of the optical afterglow properties, and therefore will allow us to study the properties of the *Swift* population in a relatively unbiased manner. Secondly, nearly all events contain multicolor ($g' R_C i' z'$) observations that allow us to evaluate the importance of host galaxy extinction for a fraction of our sample. Altogether, we aim to discriminate between the competing hypotheses proffered to explain dark GRB afterglows in the *Swift* era.

Throughout this work, we adopt a standard ΛCDM cosmology with $h_0 = 0.71$ km s^{-1} Mpc^{-1}, $\Omega_m = 0.27$, and $\Omega_\Lambda = 1 - \Omega_m = 0.73$ (Spergel et al. 2007). We define the flux density power-law temporal and spectral decay indices α and β as $f_\nu \propto t^{-\alpha}\nu^{-\beta}$ (e.g., Sari et al. 1998). All errors quoted are 1σ (i.e., 68%) confidence intervals unless otherwise noted.

2. OBSERVATIONS AND DATA REDUCTION

The P60-*Swift* early optical afterglow catalog is shown in Table 1. Here, we have included all optical afterglows of events localized by *Swift* in the three year period from 2005 April 1–2008 March 31 (roughly coinciding with the beginning of real-time GRB alerts and narrow-field instrument follow up) for which we began P60 observations within 1 hr after the BAT trigger.

All P60 data were reduced in the IRAF[10] environment using our custom real-time reduction pipeline (Cenko et al. 2006a). Where necessary, coaddition was performed using SWarp.[11] For the vast majority of events, magnitudes were calculated using aperture photometry with the inclusion radius roughly matched to the stellar point-spread function FWHM. For the few events with either extremely crowded fields or variable, elevated backgrounds (due to nearby bright stars or the moon), image subtraction was performed using the ISIS package (Alard & Lupton 1998).

Photometric calibration was performed relative to the SDSS data release 6 (Adelman-McCarthy et al. 2008) where possible, typically resulting in rms variations of $\lesssim 0.05$ mag in all filters. For those fields without Sloan coverage, we made use of the calibration files provided by A. Henden[12] when

[10] IRAF is distributed by the National Optical Astronomy Observatory, which is operated by the Association for Research in Astronomy, Inc., under cooperative agreement with the National Science Foundation.
[11] See http://terapix.iap.fr/soft/swarp.
[12] Available via ftp at ftp.aavso.org.

Table 2
P60 Filter Reference

P60 Filter	Central Wavelength[a] (Å)	Reference Filter	Photometric System	Zeropoint[a] (Jy)
g	4927	g'	AB	3631
V_C	5505	V_C	Vega	3590
R_C	6588	R_C	Vega	3020
i'	7706	i'	AB	3631
i	7973	I_C	Vega	2380
I_C	8060	I_C	Vega	2380
z	9133	z'	AB	3631
z'	9222	z'	AB	3631

Note. [a] Reference: Fukugita et al. (1995).

available, resulting in similar quality calibrations to the SDSS. The remaining events were calibrated relative to the USNO-B1 catalog,[13] resulting in significantly poorer zero-point fits. Particularly in the g, z, and z' filters, the rms errors for these events could be quite large (~ 0.6 mag). Photometric and instrumental errors have been added in quadrature to obtain the results presented in Table 1.

Filter transformations (either from the Johnson–Kron–Cousins Vega system to the SDSS AB system, or vice versa) were made using the results from Jordi et al. (2006). Throughout this work, the Gunn g and z filters have been calibrated relative to the SDSS g' and z' filters, and their corresponding magnitudes are reported in the AB system. The Gunn i filter, used for some early observations in 2005, was found to best match the Cousins I_C filter, and hence is reported on the Vega system. The remaining filters have magnitudes reported in their native photometric system (i.e., Vega for V_C, R_C, and I_C, and AB for i' and z'). A summary of the relevant photometric calibration and appropriate zero point for flux conversion can be found in Table 2. Full throughput curves for all P60 filters can be found in Cenko et al. (2006a).

Finally, we note that the magnitudes reported in Table 1 have not been corrected for Galactic extinction along the line of sight. For all subsequent figures and analysis, this correction has been applied using the dust extinction maps of Schlegel et al. (1998) and the Milky Way extinction curve from Cardelli et al. (1989). For most bursts, the extinction correction was quite small [$\langle E(B-V)\rangle = 0.04$ mag], although a few events were subjected to large column densities [e.g., GRB 060110: $E(B-V) = 0.97$ mag]

3. ANALYSIS

The standard theoretical paradigm to explain GRBs is the relativistic fireball model (e.g., Piran 2005). In the case of long-duration GRBs, accretion onto the black hole remnant of massive star core collapse powers an ultrarelativistic outflow of matter and/or radiation (Woosley 1993). Shocks and/or instabilities within the outflow generate the prompt γ-rays (i.e., internal shocks). The afterglow emission, on the other hand, is powered by electrons in the circumburst medium accelerated by the outgoing blast wave (i.e., external shocks). The resulting synchrotron spectrum and light curve are well described by a series of broken power laws (Granot & Sari 2002), with the break frequencies determined not only by properties of the outflow (E, θ, etc.), but also by the nature of the circumburst medium. In what follows we attempt to understand the early optical afterglow phase in the context of this model.

[13] See http://www.nofs.navy.mil/data/fchpix.

The R_C-band optical light curves (and upper limits) for all 29 events in the P60-*Swift* early optical afterglow sample are shown in Figure 1. For all events with P60 optical detections, we have simultaneously fit both the spectral and temporal evolution of the light curve, assuming a power-law spectrum and either a single or broken power-law temporal evolution. The results of this analysis are shown in Table 3.

Because afterglow emission is a broadband phenomenon, multiwavelength observations can often provide important constraints that would be overlooked by considering only a single bandpass. We have therefore obtained XRT light curves from the on-line *Swift*-XRT light curve repository[14] (Evans et al. 2007). We converted the 0.3–10 keV fluxes to flux densities at a nominal energy of 2 keV assuming a power-law X-ray spectrum with indices provided in the Gamma-Ray Burst Coordinate Network (GCN)[15] circulars. We then fit the temporal decay of each X-ray light curve, assuming either a single or broken power-law model.

With these results in hand, we now move on to explore the anomalously large P60 detection efficiency (Section 3.1); the relationship between X-ray and optical flares (Section 3.2); the brightness and luminosity distribution of *Swift* optical afterglows (Section 3.3); and optically dark bursts in the *Swift* era (Section 3.4).

3.1. Detection Efficiency

The most striking feature in Table 3 is the large fraction of P60 detected afterglows: of the 29 events in the sample, P60 detected 22 (76%). This stands in stark contrast with the 32% afterglow detection efficiency of the UVOT (Roming et al. 2006) and even exceeds the 50% value reported by the larger Liverpool and Faulkes telescopes (Melandri et al. 2008). For those events without P60 detections, one (GRB 050607: Rhoads 2005) was detected in the optical below our sensitivity limits, while three were detected in the NIR (GRB 050915A: Bloom & Alatalo 2005; GRB 060923A: Tanvir et al. 2006; GRB 061222A: Cenko & Fox 2006). Only three events (10%) in the entire sample registered no detections in the optical or NIR bandpass: GRBs 050412, 060805, and 070521.

59% of the events in the sample (17 of 29) have a redshift measured from optical spectroscopy, roughly a factor of 2 larger than the *Swift* population as a whole. These range from $z = 0.6535$ (GRB 050416A; Soderberg et al. 2007) to $z = 4.9$ (GRB 060510B; Price et al. 2007). Together with our measured median redshift of $\langle z\rangle \approx 2$, the events in our sample are relatively representative of *Swift* afterglows ($\langle z\rangle \approx 2.0$; Berger

[14] See http://www.swift.ac.uk/xrt_curves.
[15] See http://gcn.gsfc.nasa.gov/gcn3_archive.html.

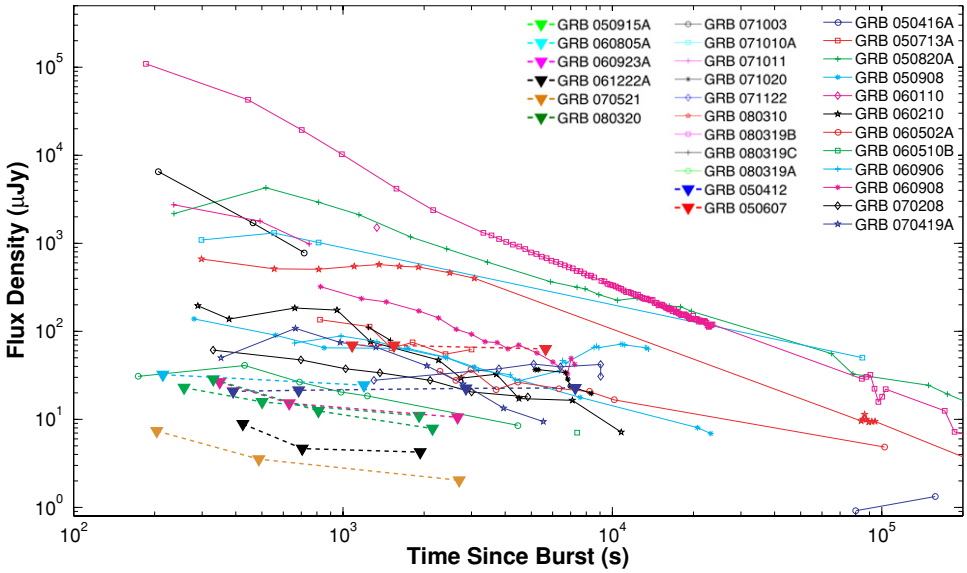

Figure 1. P60-*Swift* early optical afterglow sample. We plot here R_C-band light curves or upper limits for all 29 events in the P60-*Swift* early optical afterglow sample. With the exception of GRB 050607, the upper limits fall securely at the very faint end of the distribution (see also Figure 4).

(A color version of this figure is available in the online journal.)

et al. 2005; Jakobsson et al. 2006b). We wish to reiterate here again that P60 immediately responds to all *Swift* events visible at the Palomar Observatory (weather permitting), ruling out any large selection bias. While small number statistics may account for some of our observed deviations from previous studies, our large detection efficiency merits a more thorough discussion in Section 4.1.

3.2. X-ray and Optical Flares

A large fraction ($\approx$ 33%) of *Swift* X-ray light curves exhibit dramatic short-lived flares superposed on their power-law decay (Falcone et al. 2007). The temporal and spectral structure of these flares indicate they cannot come from the external shock powering the afterglow emission; instead they are widely attributed to late-time activity of the central engine (Zhang et al. 2006). Likewise, a re-brightening at late times in the optical bandpass has now been seen in several *Swift* afterglows (Woźniak et al. 2006; Stanek et al. 2007). Investigating the relationship between these two bandpasses should help shed light on the emission mechanisms responsible for these deviations from standard afterglow theory.

Our early afterglow sample includes four events with contemporaneous optical observations of X-ray flares: GRBs 050820A, 050908, 060210, and 080310 (Figures 2 and 3). The relationship between the X-ray and optical emission from GRB 050820A is discussed extensively in Cenko et al. (2006b) and Vestrand et al. (2006). While the optical emission clearly jumps in concert with the bright X-ray flare at $t \approx 230$ s,[16] the dominant contribution to the optical emission at later times appears to come from the forward shock. In the other three events, the optical emission is completely decoupled from any flaring in the X-rays.

GRB 060906 is unique in our sample, as we observe a re-brightening by a factor of ≈ 3 at $t \approx 10^4$ s in the optical. The X-ray decay, on the other hand, appears relatively flat during this stage. One possibility of explaining the optical flare is an increase in the circumburst density; such a change in the surrounding medium should have no effect on any emission above the synchrotron cooling frequency, ν_c, where the X-ray bandpass is likely to fall. However, a recent study by Nakar & Granot (2007) has shown that even sharp density changes do not lead to dramatic variability in afterglow light curves; instead any changes in the afterglow evolution occurs smoothly over several orders of magnitude in time. We leave a more thorough discussion of the afterglow of GRB 060906 to V. R. Rana et al. (2009, in preparation).

3.3. Brightness and Luminosity Distribution

We have interpolated (where possible) or extrapolated the R_C-band flux (corrected for Galactic extinction) to a common time of $t = 10^3$ s in the observer frame for 21 P60-detected afterglows in our sample.[17] A plot of the resulting cumulative distribution is shown in Figure 4. For those events without detections, we take the deepest upper limit obtained before this fiducial time, and plot this limit as an arrow in Figure 4. For comparison, we also show the analogous result obtained by Akerlof & Swan (2007) in a literature-based study of the first 43 *Swift* optical afterglows from 2005 to 2006.

It is clear from the large degree of overlap in the two distributions in Figure 4 that our sample, though slightly smaller in size, is consistent with the findings of Akerlof & Swan (2007) and therefore likely representative of the entire *Swift* optical afterglow population. We find a slight degree of variation at the faint end ($R_C \gtrsim 21.5$ mag), which likely indicates we are missing a small fraction ($< 10\%$) of the faintest afterglows. However, given that $\sim$ 70% of *Swift* events seem to have $R_C < 22$ mag at this fiducial time (Akerlof & Swan 2007), the P60 sensitivity is well matched to detect the majority of events.

For those events for which we do not detect an optical afterglow with P60, it is clear from Figures 1 and 4 that only one event can be attributed to a lack of sensitivity (GRB 050607, which was located only 3″ from a $R \approx 16$ mag star). The

[16] Note this "flaring" is actually likely the main portion of the prompt emission, as *Swift* triggered on a faint precursor for this event. See Cenko et al. (2006b) for details.

[17] GRB 080320 was only detected in the i' and z' filters and is therefore included in Figure 4 as a limit.

Table 3
P60-*Swift* Early Optical Afterglow Sample

GRB Name	P60 OT?	Other OT/IRT?[a]	Redshift[b]	α_1[c]	α_2[c]	t_b[c] (10^3 s)	β_O[c]	χ^2_r (d.o.f.)[c]	β_{OX}[d]	A_V(host)[e] (mag)
050412	No	No	...	...	...	...	...	...	< 0.49	...
050416A	Yes	...	0.6535	0.23 ± 0.08	$0.9^{+2.0}_{-0.3}$	$11.6^{+66.6}_{-8.9}$	2.6 ± 1.8	1.33 (7)	0.35	...
050607	No	OT	...	...	...	...	...	...	< 0.72	...
050713A	Yes	...	...	$0.62^{+0.12}_{-0.11}$	...	...	...	0.72 (7)	0.31	...
050820A[f]	Yes	...	2.615	...	...	...	...	...	0.40	< 0.10
050908	Yes	...	3.35	0.69 ± 0.05	...	...	-0.4 ± 1.1	0.75 (12)	0.91	...
050915A	No	IRT	...	...	...	...	...	...	< 0.44	...
060110	Yes	...	...	$0.92^{+0.30}_{-0.25}$	...	...	...	0.23 (8)	0.80	...
060210	Yes	...	3.91	0.93 ± 0.06	...	...	7.2 ± 0.7	1.43 (21)	0.37	$1.21^{+0.16}_{-0.12}$
060502A	Yes	...	1.51	0.49 ± 0.05	...	...	2.1 ± 0.3	0.42 (24)	0.53	0.53 ± 0.13
060510B	Yes	...	4.9	0.3 ± 0.5	...	...	$4.2^{+1.8}_{-2.2}$	0.15 (4)	0.04	...
060805A	No	No	...	...	...	...	...	...	< 0.76	...
060906[g]	Yes	...	3.685	...	...	...	2.2 ± 0.2	0.22 (20)	0.88	$0.20^{+0.01}_{-0.12}$
060908	Yes	...	2.43	1.03 ± 0.02	...	...	0.46 ± 0.06	2.26 (52)	0.82	...
060923A	No	IRT	...	...	...	...	...	...	< 0.41	...
061222A	No	IRT	...	...	...	...	...	...	< 0.15	...
070208	Yes	...	1.165	0.50 ± 0.02	...	...	2.18 ± 0.12	1.81 (23)	0.54	0.96 ± 0.09
070419A	Yes	...	0.97	-2.7 ± 0.6	1.04 ± 0.04	0.53 ± 0.02	1.5 ± 0.2	2.57 (17)	0.87	$0.70^{+0.31}_{-0.11}$
070521	No	No	...	...	...	...	...	...	< -0.03	...
071003	Yes	...	1.60435	1.77 ± 0.05	...	...	0.86 ± 0.19	0.48 (8)	0.27	< 0.26
071010A	Yes	...	...	0.29 ± 0.19	...	...	1.2 ± 0.7	0.85 (6)	0.83	...
071011	Yes	...	...	0.90 ± 0.20	...	...	1.9 ± 0.7	0.26 (6)	0.66	...
071020	Yes	...	2.145	0.89 ± 0.12	...	...	0.58 ± 0.27	2.16 (14)	0.52	...
071122	Yes	...	1.14	-0.08 ± 0.09	...	...	1.3 ± 0.6	0.36 (11)	0.64	0.58 ± 0.05
080310	Yes	...	2.43	0.03 ± 0.03	0.69 ± 0.07	1.83 ± 0.02	0.97 ± 0.06	0.55 (24)	0.79	0.10 ± 0.02
080319A	Yes	...	...	-0.9 ± 0.4	0.80 ± 0.07	$0.160^{+0.136}_{-0.070}$	2.0 ± 0.3	1.50 (11)	0.41	...
080319B	Yes	...	0.937	$1.93^{+0.04}_{-0.06}$	1.238 ± 0.004	10.10 ± 0.17	0.50 ± 0.02	0.57 (280)	0.52	...
080319C	Yes	...	1.95	1.4 ± 0.2	...	...	2.4 ± 0.2	2.32 (3)	0.36	0.67 ± 0.06
080320	Yes	...	...	...	...	...	...	...	< 0.31	...

Notes.

[a] Optical (OT) and Infrared (IRT) transient references: GRB 050607: Rhoads (2005); GRB 050915A: Bloom & Alatalo (2005); GRB 060923A: Tanvir et al. (2006); GRB 061222A: Cenko & Fox (2006).

[b] Redshift references: GRB 050416A: Soderberg et al. (2007); GRB 050820A: Prochaska et al. (2008b); GRB 050908: Fugazza et al. (2005); GRB 060210: Cucchiara et al. (2006a); GRB 060502A: Cucchiara et al. (2006b); GRB 060510B: Price et al. (2007); GRB 060906: Jakobsson et al. (2006a); GRB 060908: Rol et al. (2006); GRB 070208: Cucchiara et al. (2007b); GRB 070419A: Cenko et al. (2007); GRB 071003: Perley et al. (2008); GRB 071020: Jakobsson et al. (2007); GRB 071122: Cucchiara et al. (2007a); GRB 080310: Prochaska et al. (2008a); GRB 080319B: Vreeswijk et al. (2008); GRB 080319C: Wiersema et al. (2008).

[c] We fitted the flux density to a single or broken power-law model of the form $F_\nu = t^{-\alpha}\nu^{-\beta}$.

[d] The optical-to-X-ray spectral index, measured at $t = 10^3$ s.

[e] We fitted for the host galaxy reddening by fixing the spectral index to $\beta = 0.6$ and assuming an SMC-like extinction law (Pei 1992).

[f] The optical light curve of GRB 050820A consists of many power-law segments. See Cenko et al. (2006b) for details.

[g] The optical light curve of GRB 060906 is not well described by either a single or broken power-law. The spectral index was calculated over only a small period of relatively flat evolution ($t > 10^4$ s).

remaining six events would all have been easily detected if as bright as a typical afterglow in our sample.

For the 17 GRBs with redshifts, it is also possible to compare optical light curves in the GRB rest frame. We therefore compute the afterglow luminosity at a fiducial time of 10^3 s in the rest frame of the GRB, applying a k-correction to convert our observed bandpass to the rest frame R_C band, as described in Hogg et al. (2002). The resulting histogram is shown in Figure 5. At this time, we find a median value for the afterglow luminosity to be $\langle \log(L[\mathrm{erg}^{-1}]) \rangle = 46.39$ with a standard deviation of 1.4 dex. Also shown in Figure 5 is the best-fit single Gaussian distribution.

Several authors (Liang & Zhang 2006; Nardini et al. 2006; Kann et al. 2006) have argued in favor of a bimodal distribution of intrinsic afterglow luminosity, with a class of nearby, subluminous events. Much like Melandri et al. (2008), we find no need for a bimodal distribution, although we caution that our distribution was calculated at an earlier time in the rest frame than previous studies. While a single event (GRB 060210) is a significant outlier on the overluminous end, we note this event is at a relatively high redshift ($z = 3.91$; Cucchiara et al. 2006a) and has an extremely steep spectral index ($\beta = 7.2 \pm 0.7$). The resulting k-correction is therefore extremely large (and relatively uncertain). This seems a more likely explanation than such an extremely luminous burst.

3.4. Dark Bursts

We adopt here the definition of a "dark" GRB as one where the optical ($R_C$band) to X-ray spectral index satisfies $\beta_{OX} < 0.5$ (Jakobsson et al. 2004). Unlike definitions based solely on optical brightness, the β_{OX} method is physically motivated: an afterglow qualifies as dark when the ratio of optical to X-ray flux is incompatible with standard synchrotron afterglow theory. By utilizing both the optical and X-ray afterglows, we can easily distinguish between intrinsically subluminous afterglows

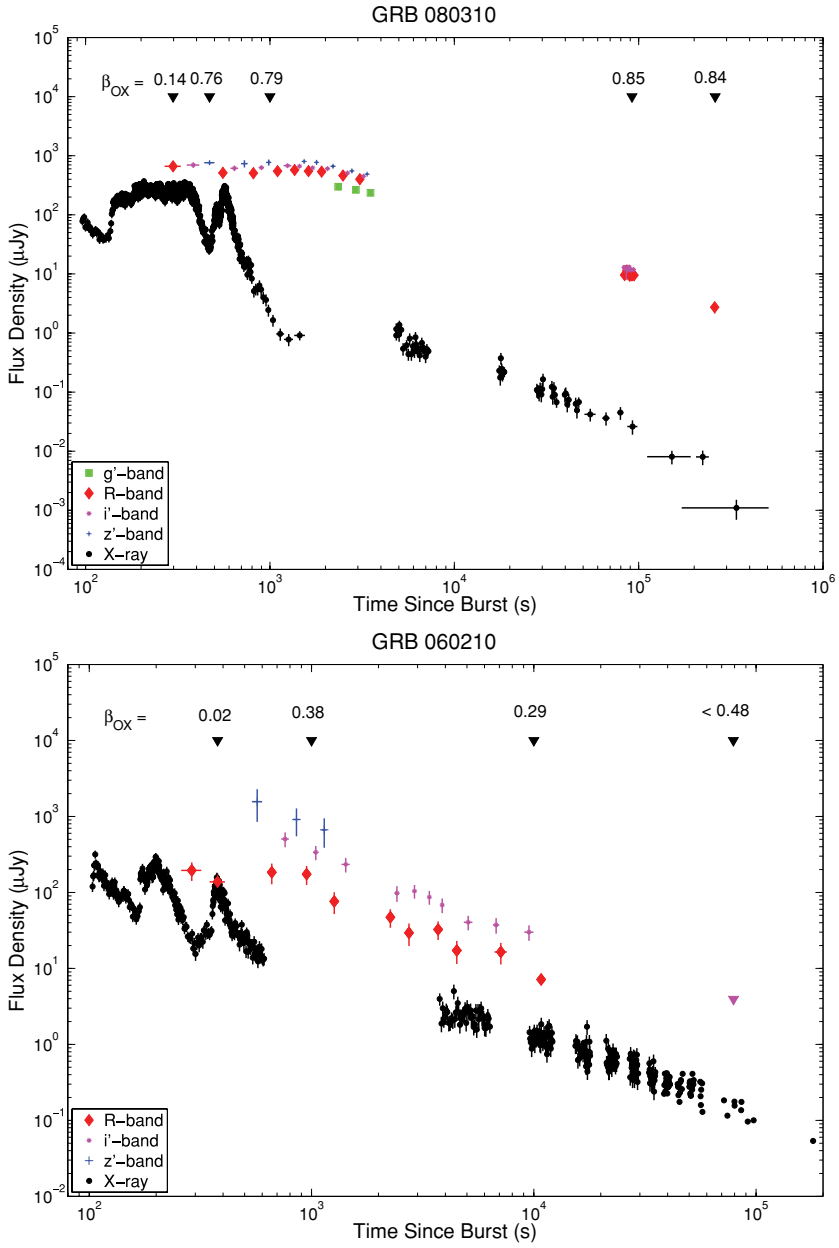

Figure 2. X-ray and optical light curves of GRB 080310 (top) and GRB 060210 (bottom). For both events the optical light curve at early times ($t \lesssim 10^3$ s) is not correlated with the dramatic X-ray flares. Measurement of the optical to X-ray spectral index (β_{OX}; Section 3.4) is therefore a strong function of time. Measuring β_{OX} during an X-ray flare may lead to erroneous classification of some bursts as "dark" ($\beta_{OX} < 0.5$). Both events, however, show relatively constant β_{OX} values for $t \gtrsim 10^3$ s. GRB 060210, for example, is clearly a dark burst, even at late times.

(A color version of this figure is available in the online journal.)

(i.e., those events that are faint in all bandpasses) and those afterglows that indicate an additional process is selectively suppressing the optical flux (or, alternatively, increasing the X-ray emission).

In Figure 6 we compare the X-ray and R_C-band flux densities extrapolated to a common time of $t = 10^3$ s for all 29 afterglows in our sample. The allowed region in the standard afterglow model, $0.50 \lesssim \beta_{OX} \lesssim 1.25$, is marked with solid lines. Like Melandri et al. (2008), we find that nearly 50% of events qualify as dark under this definition. It is clear therefore that the faintness of the *Swift* optical afterglows cannot be attributed solely to distance, as this would not directly affect the measured flux ratio. This result stands in stark contrast with the study of pre-*Swift* events by Jakobsson et al. (2004), which found a dark burst incidence of only 10%.

The most important difference between our study and that of Jakobsson et al. (2004) is the time at which we evaluate β_{OX} ($t = 11$ hr for Jakobsson et al. 2004). In Figure 2 we demonstrate the importance of the reference time when calculating β_{OX}. Many *Swift* afterglows exhibit bright X-ray flares at early times (Burrows et al. 2005b), as well as a plateau decay phase indicative of continued energy injection into the forward shock (Nousek et al. 2006; Zhang et al. 2006). This late-time activity could artificially inflate the X-ray flux at early times, leading to spuriously low β_{OX} measurements (see GRB 080310, Figure 2).

While our optical coverage at $t = 11$ hr is relatively sparse, we find little evidence for evolution of β_{OX} between these two epochs. Delayed engine activity may explain the low values of β_{OX} measured for a few events (e.g., GRB 050820A; Cenko

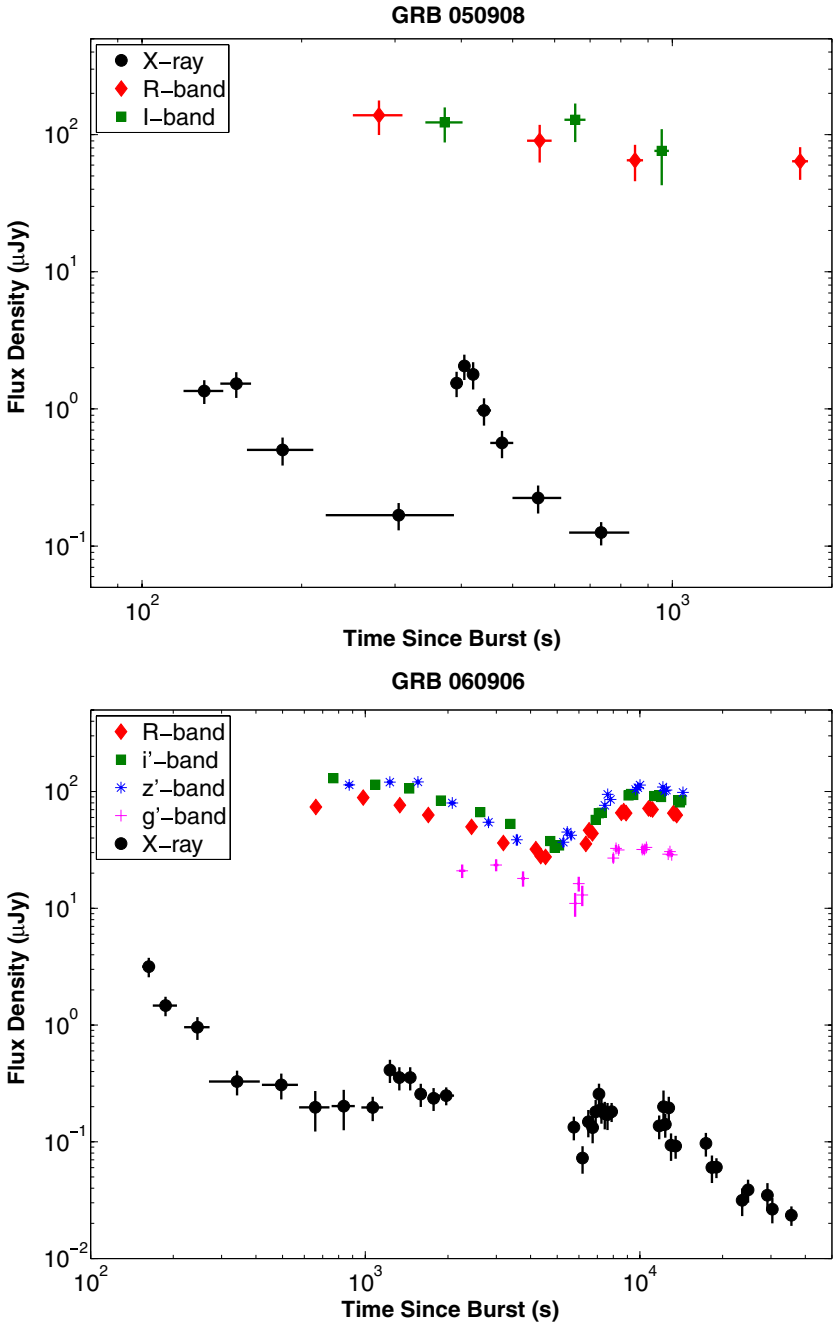

Figure 3. X-ray and optical flares in *Swift* afterglows. Top: X-ray and optical light curves of GRB 050908. The X-ray light curve shows a dramatic flare ($\Delta f/f \approx 50$ at $t \approx 400$ s) at early times. No corresponding variability is seen in the optical. Bottom: X-ray and optical light curves of GRB 060906. In this case, the re-brightening occurs in the optical while the X-ray decay is relatively flat. Both events require additional emission mechanisms beyond the forward shock synchrotron model.
(A color version of this figure is available in the online journal.)

et al. 2006b). But we find that extrapolating the light curves out to both $t = 10^4$ s and $t = 11$ hr does not change the dark burst fraction by more than 10%. This echoes the result found by Melandri et al. (2008).

Another possibility to explain dark optical afterglows is a high-redshift ($z \gtrsim 5$) origin. In this case, the observed R_C band-pass falls below the Ly-α cut-off in the GRB rest frame, leading to a significant suppression of optical flux due to absorption in the IGM. This is the case, for example, for GRB 060510B ($\beta_{OX} = 0.04$), which lies at $z = 4.9$ (Figure 6; Price et al. 2007).

Much like the delayed engine activity hypothesis, a high-redshift origin can only account for a fraction of the observed dark bursts in our sample. Theoretical models, assuming GRBs trace the cosmic star formation rate, predict a high-redshift ($z \gtrsim 7$) fraction of $\approx 10\%$ (Bromm & Loeb 2006). Five events with $\beta_{OX} < 0.5$ have measured spectroscopic redshifts, firmly establishing the Ly-α cut-off below the observed R_C filter (e.g., GRB 060210: $\beta_{OX} = 0.37$, $z = 3.91$; Cucchiara et al. 2006a). And we can place probabilistic upper limits on the redshifts of some events that do not have optical afterglows based on the inference of absorption in excess of the Galactic value in X-ray afterglow spectra (e.g., GRB 070521A: $z < 2.4$; Grupe et al. 2007).

Finally, we consider the possibility of extinction native to GRB host galaxies. Because long-duration GRBs have massive star progenitors, it is natural to expect them to explode in dusty,

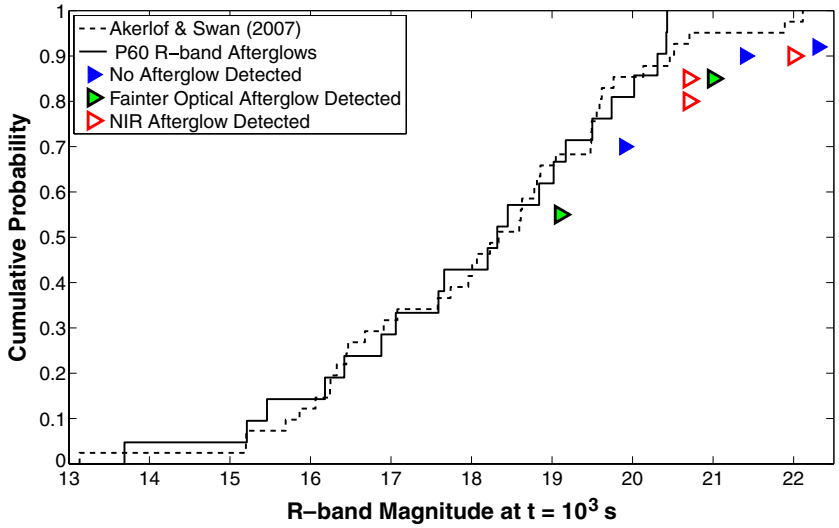

Figure 4. P60-*Swift* optical afterglow brightness distribution. We plot here the observed optical brightness distribution of all events in our early afterglow sample at a common reference time of $t = 10^3$ s (solid line). The dashed line indicates a similar archival analysis performed by Akerlof & Swan (2007). Minor deviations can be seen at the very faint end ($R_C \gtrsim 21$ mag), likely indicative of the P60 sensitivity limit. Arrows indicate P60 upper limits for GRBs with optical afterglows from other facilities (green), GRBs with only NIR afterglows (red), and GRBs with no detected optical or NIR afterglows (blue).

(A color version of this figure is available in the online journal.)

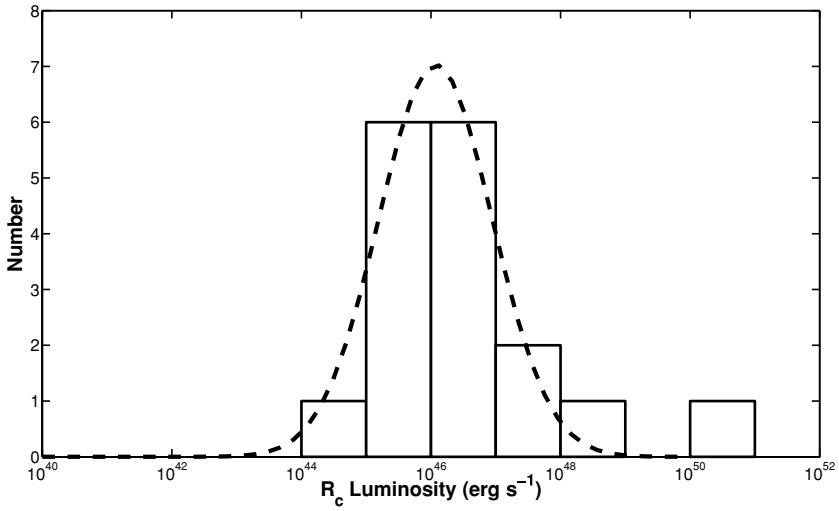

Figure 5. P60-*Swift* optical afterglow luminosity distribution. We have measured the rest frame optical R_C-band luminosity at a common (rest frame) time of $t = 10^3$ s for all events in our early sample with a spectroscopic redshift. We find a good fit to a single log-normal distribution with mean $\log(L[\mathrm{erg}^{-1}]) = 46.68$ and standard deviation $\sigma = 1.04$ dex. The sole outlier (GRB 060210) falls on the overluminous end because of its extreme k-correction (Section 3.3).

highly extinguished environments. However, broadband studies of some of the best sampled afterglows in both the pre-*Swift* and *Swift* eras indicate only a modest amount of host reddening ($\langle A_V \rangle \approx 0.2$ mag; Kann et al. 2006, 2007).

In contrast, we find evidence for significant host absorption in several of the afterglows in our sample. Using our multicolor P60 observations, we provide best-fit optical power-law spectral indices for all events with sufficient filter coverage in Table 3. Of the seven dark bursts with measured values of β_O, six spectral indices are too steep to be explained by the standard afterglow formulation (i.e., $\beta_O > 1.5$).

To further quantify this effect, we have refitted our optical data, but in this case fixing the optical spectral index to $\beta_O = 0.6$ (the average value for bright *Swift* events; Kann et al. 2007). We then incorporated the effects of dust by adding the host galaxy reddening [A_V(host)] as a free parameter to the fit. In general, our data were not sufficient to distinguish between competing extinction laws (i.e., Milky Way, LMC, and SMC; Pei 1992). We therefore assumed an SMC-like extinction curve, as this model has proved successful for most GRB afterglows. The results are shown in Table 3. The extinction-corrected fluxes are also plotted in Figure 6. In all cases where we were able to measure the host extinction, this correction has moved the afterglow from near or below the dark burst threshold back into the realm of synchrotron theory.

It is clear that the afterglows in our sample are significantly more reddened than the brightest afterglows in both the *Swift* and pre-*Swift* eras. Furthermore, even our host absorption measurements are quite biased; we could not measure A_V(host) for those events without P60 afterglows, which are likely to be the most extinguished events in our sample. Even some afterglows that do not qualify as dark, such as GRB 070208 and GRB 070419A, exhibit strong evidence for significant amounts of host galaxy dust [A_V(host) $\geqslant 0.7$]. Though our sample size is still quite small, host galaxy extinction appears to be the primary explanation for dark bursts in the *Swift* era.

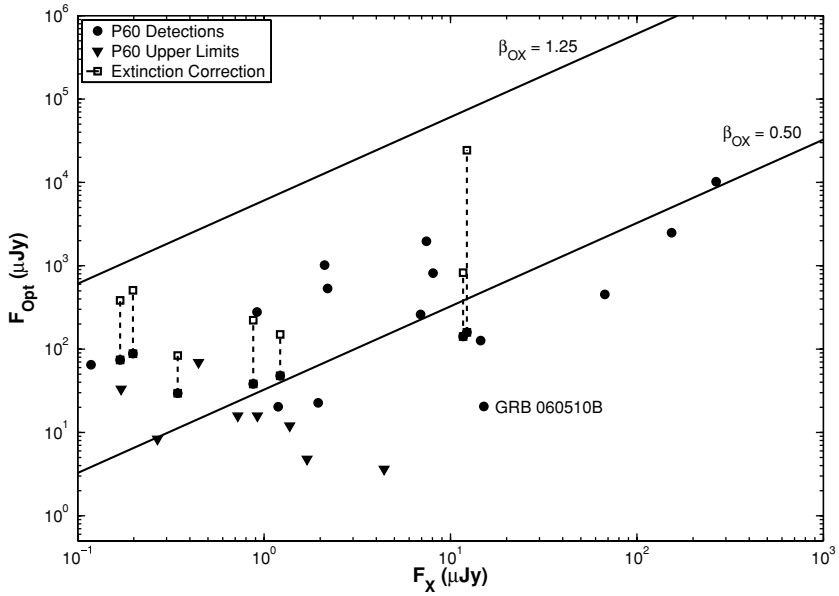

Figure 6. Optical/X-ray spectral energy distribution of *Swift* GRBs. We plot the X-ray and optical flux (or upper limits) at a common reference time of $t = 10^3$ for all events in our P60-*Swift* sample. In standard afterglow theory, the optical to X-ray spectral index, β_{OX} should fall between $0.5 < \beta_{OX} < 1.25$ (solid black lines). In our sample, nearly 50% of afterglows qualify as "dark" bursts ($\beta_{OX} < 0.5$). Correcting for extinction in the GRB host galaxy (open squares) brings several events in line with the predictions of synchrotron radiation.

4. DISCUSSION AND CONCLUSIONS

4.1. Anomalous P60 Detection Efficiency

We have demonstrated in Section 3.1 that P60 was able to detect optical afterglow emission from a large fraction ($\sim$ 80%) of events for which observations began within an hour of the burst trigger. While the 1.5 m aperture is relatively large for a robotic facility, it would be nonetheless informative to understand systematic effects that affect our afterglow recovery rate. The ultimate goal, of course, is to better inform future GRB follow-up campaigns.

The first lesson from this campaign is the importance of observing in redder filters. We have shown in Section 3.4 that typical *Swift* events suffer from a non-negligible amount of host galaxy extinction (Table 3). Coupled with the additional effect of Ly-α absorption in the IGM from a median redshift of $\langle z \rangle \approx 2$, it is clear that a large fraction of the low UVOT detection efficiency is caused by its blue observing bandpass. The P60 automated follow-up sequence, consisting of alternating exposures in the R_C, i', and z' filters, while initially designed for identification of candidate high-z events, is actually well suited to maximize afterglow detection rates.

The large fraction of P60-detected bursts with spectroscopic redshifts, on the other hand, is almost certainly an artifact of the unequal longitudinal distribution of large optical telescopes. Nearly all optical telescopes with apertures larger than 8 m fall within six time zones (UT-4 to UT-10). It is not entirely surprising then that so many promptly discovered P60 optical afterglows have spectroscopic redshifts from immediate follow up with the largest optical facilities.

While building the largest optical facilities is often prohibitively expensive for all but the largest collaborations, 1 m class facilities are much more feasible, both in terms of cost and construction timescale. We wish here to echo the thoughts of many previous GRB observers (e.g., Akerlof & Swan 2007) that future automated facilities be built at longitudes (and latitudes) not covered by current facilities. NIR coverage is particularly crucial to detect the most extinguished events and provide tighter constraints on the afterglow SED and hence host galaxy extinction.

A longitudinally spaced ring of 1 m class facilities, as for example envisioned by the Las Cumbres Observatory Global Telescope[18] is well positioned in the future to recover the vast majority of GRB optical afterglows, assuming the follow up is done in the reddest filters possible. Such coverage will be particularly important as we transition into the *Fermi* era, with its significantly decreased rate of precise GRB localizations.

4.2. Re-visiting Dark Bursts

We now turn our attention to the issue of dark bursts in the *Swift* era. In Section 3.4, we demonstrated that a large fraction ($\approx$ 50%) of *Swift* afterglows showed suppressed emission in the optical bandpass (relative to the X-ray), which was due in large part to extinction in the host galaxy. Given the natural expectation that GRBs, since they are associated with massive stars, should form in relatively dusty environments, we wish to understand why our study of *Swift* events yields such a dramatically different dark burst fraction than previous work on pre-*Swift* GRBs (Jakobsson et al. 2004).

We believe selection effects are one large cause of this discrepancy. It is clear that previous studies of GRB host galaxy extinction, by selecting the brightest and best-sampled events, provide a strongly biased view. Many, if not most, GRB hosts, appear to suffer from a significant amount of dust extinction ($A_V \gtrsim 0.5$). Even the study of Jakobsson et al. (2004), though it included *all* pre-*Swift* GRBs with an X-ray afterglow, could be biased toward unextinguished events as well. Before *Swift*, target-of-opportunity X-ray observations often required the accurate localization provided by an optical (or radio) afterglow. Thus those events with the brightest optical afterglows (assumed to have on average smaller extinction) were more likely to be observed in the X-ray, biasing the optical-to-X-ray spectral index to larger values of β_{OX}.

[18] See http://lcogt.net.

Another, more subtle, effect, may also cause *Swift* afterglows to appear darker than pre-*Swift* afterglows, independent of host galaxy extinction. Because *Swift* is a more sensitive instrument, it detects GRBs at a higher average redshift than any previous mission. Consider a host frame extinction of $A_V = 0.1$ mag. At $z = 1$, typical for pre-*Swift* events, the observed R_C filter corresponds roughly to rest-frame U band, and so an extinction of 0.17 mag (assuming a Milky Way like extinction curve). On the other hand, at $z = 3$, the observed R_C band corresponds to a rest frame wavelength of $\lambda = 1647$ Å. So at high redshift, the same amount of dust will produce nearly twice as much extinction in the observed bandpass. Solely because of redshifts effects, similar environments will produce different observed spectral slopes. This effect is exacerbated by the nature of dust grains in most GRB host galaxies, as the SMC extinction curve shows significantly larger extinction in the rest frame far-UV than a Milky Way like galaxy (Pei 1992).

If GRBs do trace the cosmic star-formation rate, our results suggest a significant fraction of star formation occurs in highly obscured environments. Kann et al. (2006) found a weak correlation between host reddening and sub-mm flux, and we believe a sensitive mid-infrared or sub-mm survey of GRB host galaxies would be an important confirmation of our results. However, instead of focusing on the brightest, best studied afterglows, as has often been done in the past (e.g., Tanvir et al. 2004; Michałowski et al. 2008), we instead suggest a survey of the host galaxies of the optically darkest GRB afterglows to see if these events really do exhibit signs of obscured star formation.

We wish to thank D. A. Kann for valuable comments on this manuscript. P60 operations are funded in part by NASA through the *Swift* Guest Investigator Program (Grant Number NNG06GH61G). S.B.C. was supported by a NASA Graduate Student Research Program Fellowship at Caltech, and acknowledges support from Gary and Cynthia Bengier, as well as from Richard and Rhoda Goldman, to the research of Alex Filippenko's group at U.C. Berkeley. M.M.K. would like to acknowledge the Moore Foundation for the Hale Fellowship supporting her graduate studies. A.G. acknowledges support by the Benoziyo Center for Astrophysics and the William Z. and Eda Bess Novick New Scientists Fund at the Weizmann Institute. This work made use of data supplied by the UK *Swift* Science Data Centre at the University of Leicester. This research has made use of the USNOFS Image and Catalogue Archive operated by the United States Naval Observatory, Flagstaff Station.

Facilities: PO:1.5m (), *Swift* (XRT)

REFERENCES

Adelman-McCarthy, J. K., et al. 2008, ApJS, 175, 297
Akerlof, C. W., & Swan, H. F. 2007, ApJ, 671, 1868
Alard, C., & Lupton, R. H. 1998, ApJ, 503, 325
Barthelmy, S. D., et al. 2005, Space Sci. Rev., 120, 143
Berger, E., Penprase, B. E., Cenko, S. B., Kulkarni, S. R., Fox, D. B., Steidel, C. C., & Reddy, N. A. 2006, ApJ, 642, 979
Berger, E., et al. 2005, ApJ, 634, 501
Bloom, J. S., & Alatalo, K. 2005, GRB Coordinates Network, 3984, 1
Bloom, J. S., Kulkarni, S. R., & Djorgovski, S. G. 2002, AJ, 123, 1111
Bromm, V., & Loeb, A. 2006, ApJ, 642, 382
Burrows, D. N., et al. 2005a, Space Sci. Rev., 120, 165
Burrows, D. N., et al. 2005b, Science, 309, 1833
Cardelli, J. A., Clayton, G. C., & Mathis, J. S. 1989, ApJ, 345, 245
Castro-Tirado, A. J., et al. 2007, A&A, 475, 101
Cenko, S. B., & Fox, D. B. 2006, GRB Coordinates Network, 5975, 1
Cenko, S. B., Gezari, S., Small, T., Fox, D. B., & Chornock, R. 2007, GRB Coordinates Network, 6322, 1
Cenko, S. B., et al. 2006a, PASP, 118, 1396
Cenko, S. B., et al. 2006b, ApJ, 652, 490
Covino, S., et al. 2008, MNRAS, 388, 347
Cucchiara, A., Fox, D. B., & Berger, E. 2006a, GRB Coordinates Network, 4729, 1
Cucchiara, A., Fox, D. B., & Cenko, S. B. 2007a, GRB Coordinates Network, 7124, 1
Cucchiara, A., Fox, D. B., Cenko, S. B., & Price, P. A. 2007b, GRB Coordinates Network, 6083, 1
Cucchiara, A., Price, P. A., Fox, D. B., Cenko, S. B., & Schmidt, B. P. 2006b, GRB Coordinates Network, 5052, 1
Evans, P. A., et al. 2007, A&A, 469, 379
Falcone, A. D., et al. 2007, ApJ, 671, 1921
Fruchter, A. S., et al. 2006, Nature, 441, 463
Fugazza, D., et al. 2005, GRB Coordinates Network, 3948, 1
Fukugita, M., Shimasaku, K., & Ichikawa, T. 1995, PASP, 107, 945
Gehrels, N., et al. 2004, ApJ, 611, 1005
Granot, J., & Sari, R. 2002, ApJ, 568, 820
Grupe, D., Nousek, J. A., Berk, D. E. V., Roming, P. W. A., Burrows, D. N., Godet, O., Osborne, J., & Gehrels, N. 2007, AJ, 133, 2216
Haislip, J. B., et al. 2006, Nature, 440, 181
Hjorth, J., et al. 2003, ApJ, 597, 699
Hogg, D. W., Baldry, I. K., Blanton, M. R., & Eisenstein, D. J. 2002, arXiv: astro-ph/0210394
Jakobsson, P., Hjorth, J., Fynbo, J. P. U., Watson, D., Pedersen, K., Björnsson, G., & Gorosabel, J. 2004, ApJ, 617, L21
Jakobsson, P., Vreeswijk, P. M., Hjorth, J., Malesani, D., Fynbo, J. P. U., & Thoene, C. C. 2007, GRB Coordinates Network, 6952, 1
Jakobsson, P., et al. 2006a, A&A, 460, L13
Jakobsson, P., et al. 2006b, A&A
Jordi, K., Grebel, E. K., & Ammon, K. 2006, A&A, 460, 339
Kann, D. A., Klose, S., & Zeh, A. 2006, ApJ, 641, 993
Kann, D. A., et al. 2007, arXiv:0712.2186
Kawai, N., et al. 2006, Nature, 440, 184
Lamb, D. Q., & Reichart, D. E. 2000, ApJ, 536, 1
Liang, E., & Zhang, B. 2006, ApJ, 638, L67
Melandri, A., et al. 2008, ApJ, 686, 1209
Michałowski, M. J., Hjorth, J., Cerón, J. M. C., & Watson, D. 2008, ApJ, 672, 817
Nakar, E., & Granot, J. 2007, MNRAS, 380, 1744
Nardini, M., Ghisellini, G., Ghirlanda, G., Tavecchio, F., Firmani, C., & Lazzati, D. 2006, A&A, 451, 821
Nousek, J. A., et al. 2006, ApJ, 642, 389
Pei, Y. C. 1992, ApJ, 395, 130
Perley, D. A., et al. 2008, ApJ, 688, 470
Piran, T. 2005, Rev. Mod. Phys., 76, 1143
Price, P. A., et al. 2007, ApJ, 663, L57
Prochaska, J. X., Murphy, M., Malec, A. L., & Miller, K. 2008a, GRB Coordinates Network, 7388, 1
Prochaska, J. X., et al. 2008b, ApJS, 168, 231
Rhoads, J. 2005, GRB Coordinates Network, 3527, 1
Rol, E., Jakobsson, P., Tanvir, N., & Levan, A. 2006, GRB Coordinates Network, 5555, 1
Rol, E., et al. 2007, ApJ, 669, 1098
Roming, P. W. A., et al. 2005, Space Sci. Rev., 120, 95
Roming, P. W. A., et al. 2006, ApJ, 652, 1416
Sari, R., Piran, T., & Narayan, R. 1998, ApJ, 497, L17
Schlegel, D. J., Finkbeiner, D. P., & Davis, M. 1998, ApJ, 500, 525
Soderberg, A. M., et al. 2007, ApJ, 661, 982
Spergel, D. N., et al. 2007, ApJS, 170, 377
Stanek, K. Z., et al. 2007, ApJ, 654, L21
Tanvir, N., Levan, A., Jarvis, M., & Wold, T. 2006, GRB Coordinates Network, 5587, 1
Tanvir, N. R., et al. 2004, MNRAS, 352, 1073
Tanvir, N. R., et al. 2008, MNRAS, 795
Vestrand, W. T., et al. 2006, Nature, 442, 172
Vreeswijk, P. M., et al. 2008, GRB Coordinates Network, 7444, 1
Wiersema, K., Tanvir, N., Vreeswijk, P., Fynbo, J., Starling, R., Rol, E., & Jakobsson, P. 2008, GRB Coordinates Network, 7517, 1
Wolfe, A. M., Gawiser, E., & Prochaska, J. X. 2005, ARA&A, 43, 861
Woosley, S. E. 1993, ApJ, 405, 273
Woosley, S. E., & Bloom, J. S. 2006, ARA&A, 44, 507
Woźniak, P. R., Vestrand, W. T., Wren, J. A., White, R. R., Evans, S. M., & Casperson, D. 2006, ApJ, 642, L99
Zhang, B., Fan, Y. Z., Dyks, J., Kobayashi, S., Mészáros, P., Burrows, D. N., Nousek, J. A., & Gehrels, N. 2006, ApJ, 642, 354